

# CRACK'S PROPAGATION IN SHORT STEEL FIBER REINFORCED CONCRETE. MODELING AND EXPERIMENTAL INVESTIGATION

Andrejs Krasnikovs, Olga Kononova and Andrejs Pupurs

Concrete Mechanics Laboratory, Riga Technical University, LV 1048, Riga, Latvia  
[akrasn@latnet.lv](mailto:akrasn@latnet.lv)

## ABSTRACT

In the present paper results of the short Steel Fiber Reinforced Concrete SFRC fracture process numerical modeling are validating by performed experimental tests. Structural short SFRC fracture model is based on the fibre pull-out laws (were determined experimentally). Different form fibre pull-out laws (pull-out load as a function of crack opening) for three types of available at the market steel fibers were determined experimentally. As the load carried by each fibre at a constant crack opening is known out of micro-mechanical experiments, the corresponding total bending load for a beam was calculated through equilibrium conditions. Modeling results were compared with experiments (SFRC beams were tested under three points and four points bending, experimentally were created more than 80 SFRC mixes with fiber content from 30kg/m<sup>3</sup> to 400kg/m<sup>3</sup>).

## 1. Introduction

Concrete as a composite material matrix is brittle. Adding short steel fibers we can increase the material stiffness, flexural and tensile strength, impact resistance, as well as

obtain a ductile behavior for cracked material. The use of steel fibers in concrete instead of traditional reinforcement is beneficial mostly due to simpler casting procedure. At the same time, technologically a large content of steel fibers in the concrete mix is negatively affects the mix workability. Therefore for the aim of good workability of the mix, steel fibers are limited both by their maximal content, geometry (chemical bond between steel fiber and concrete matrix is weak and fibers are anchoring in the matrix mainly geometrically and by frictional forces) and length. In

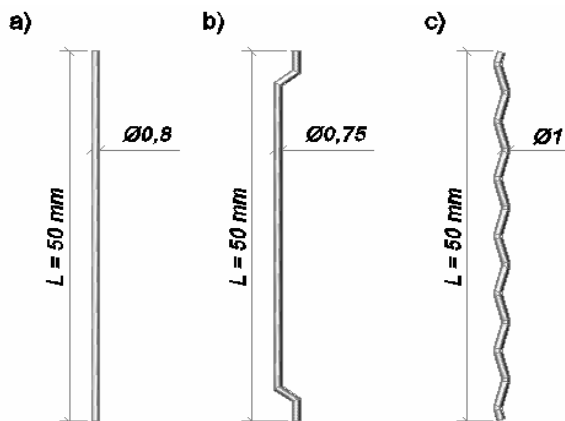


Fig.1.Types of steel fibers used in the work:  
a) straight fibre; b) Dramix fibre; c) Tabix.

traditionally reinforced concrete structures the post cracking behavior is based on the steel bars tensile strength mechanism, contrary in SFRC it is the pull-out mechanism of steel fibers that determines the load bearing capacity of the cracked material. Therefore it is important to perform a detailed micro-mechanical investigation of fibre pull-out process in order to understand and characterize the behavior and crack propagation in SFRC structural elements. Follows types of steel fibers have been used in our

investigation – straight fibers, fibers with end hooks (Dramix), and corrugated form fibers (Tabix) (see Fig.1).

## 2. Principles of the proposed model

Experimentally obtained pull-out laws (see Fig.2) were used as the main input data for the proposed model with the goal to predict linear and non-linear behavior of SFRC beams under bending loads. Beam subjected to four point bending is shown at Fig.3. SFRC beams with dimension 15x15x60 cm were cut by diamond saw at the depth of 1 cm forming the notch on the bottom side of each beam. The span length between underneath beam supports was  $L_S=50$  cm and the distance between symmetrically applied loads  $L_P=15$ cm. The main aim of the proposed model is to predict crack mouth opening displacement  $\delta$  (crack is starting from the notch) depending on applied bending load  $P$ , simultaneously obtaining load – prism upper surface midpoint vertical deflection curves.

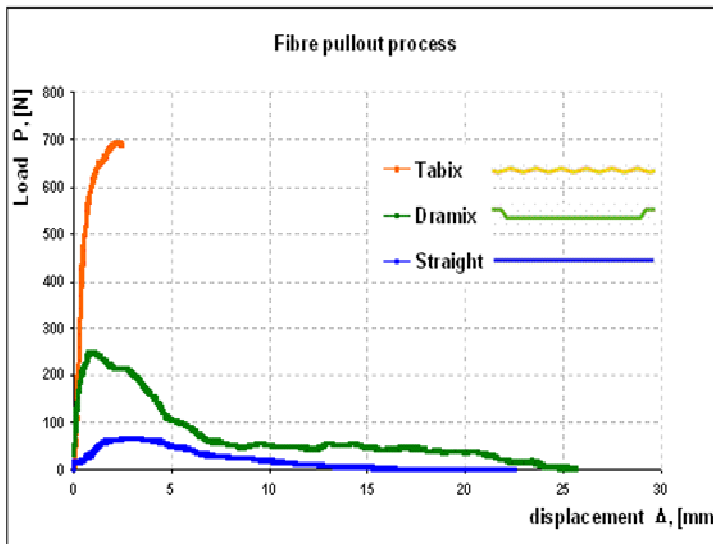


Fig. 2. The pull-out curves for different form steel fibers.

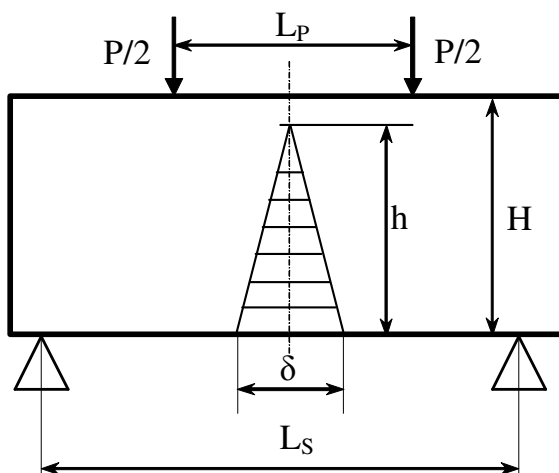


Fig. 3. SFRC beam under the four point bending conditions.

Increasing the load is applied to the beam the cracking process is starting. Micro cracks are growing and linking forming large cracks till the moment then one or more macro crack ( in our case crack was started from the notch) is crossing whole tensioned part of the beam crosssection. After the formation of the crack the tensile load is still transferred through the crack by the fibers (the bridging effect). Because the fibers are being pulled out of the concrete matrix the ability of the SFRC beam to carry the applied load in the post-cracking state purely depends on the capacity of fibers in broken crosssection to carry pull-out loads. At the same moment number of fibers crossing the crack surface is depending on fibre volume fraction in the material. According to the pull-out curves, were obtained, it follows that only for very small values of  $\delta$  fibre resistance is increasing (especially for straight and Dramix fibers), and after reaching the maximal value (see. Fig.2.), fibre resistance to withstand pull-out loads starts to decrease and thus decreases the load bearing capacity of the whole beam's broken crosssection.

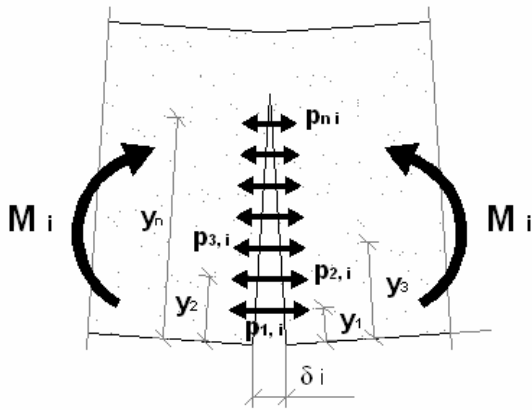


Fig. 5. Scheme of internal forces and moments formed in SFRC beam at post-cracking stage.

In the model the behavior of SFRC beam was simulated by calculating internally existing load bearing value of each fiber crossing the crack (using this fibre experimentally measured pull-out curve), depending on crack opening value  $b_i$  at the location of this particular fiber (see Fig.5.). Experimental observations shown that the total crack height is approximately constant regardless of size of the crack opening  $\delta_i$  (when  $\delta_i \in (0, 5\text{mm})$ ). At the same moment macro crack is reaching crack opening value 5mm is unstable. In average, the crack surfaces have been assumed as a plane therefore the local crack opening  $b_i$  can be simply geometrically determined from corresponding maximal crack opening  $\delta_i$ .

The iteration procedure of beam behavior modeling in bending was performed according to step sequence, with the maximal crack opening  $\delta_i$  values within the range from 0 to 6 mm.

At each step “ $i$ ” with the corresponding maximal crack opening  $\delta_i$ , firstly the local crack opening  $b_i$  is calculated as a function of distance  $y_n$ :

$$b_i = f(y_n) \quad (1)$$

As the local crack opening  $b_i$  is known at each distance  $y_n$ , the force  $p_i$  transferred

through the crack can be calculated using previously obtained fibre pull-out laws. However, this is the point when the factors of fibre embedded length, fibre volume fraction  $V_m$ , fibre orientation angle  $\alpha$  (to the crack's surface) should be evaluated, thus referring to actual properties of the material observed. The volume fraction  $V_f$  of each fibre type could be easily determined from corresponding fibre weight fraction  $W_f$ . Further, number of each type of fibers on one crack's surface was determined, as the average fibre amount crossing the crack plane with chaotic fibers orientation and embedded length distributions (were performed Monte-Carlo simulations and modeling results were compared with performed direct experimental measurements). Typical fiber pull-out force dependence curves on fiber orientation angle to crack surface are shown at Fig.6-8. The influence of fibre type, fraction and orientation actually can be summarized within one coefficient, which in this case is defined as fibre factor  $k_f$ . Now the internal force transferred through the crack can be calculated. From the pull-out curves the force  $p_{n,i}$  corresponding to a particular crack opening  $b_i$  can be determined all along the crack height as schematically depicted at Fig.5. From the calculated values of internal forces  $p_{n,i}$ , resulting bending moment  $M_i$  and corresponding external force  $P_i$  can be determined corresponding to each crack opening value  $\delta_i$ . Relation of externally applied load  $P$  as a function of crack opening displacement  $\delta$  is thus obtained at each step. The force  $P$  represents total force applied to the beam that is divided in two symmetrical forces as shown in Fig.3. To run the algorithms of the model, computer software was elaborated.

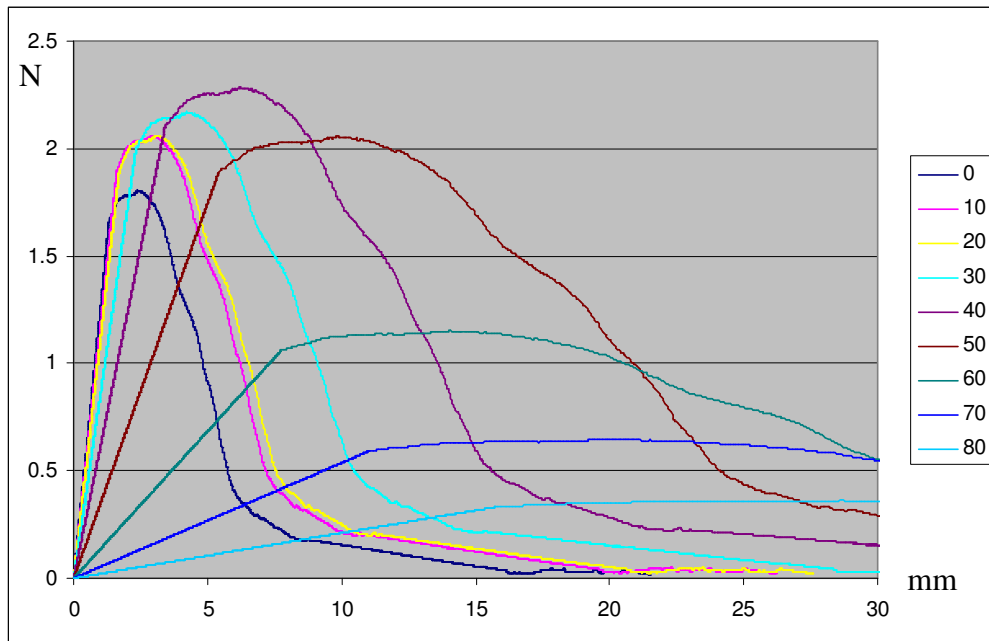


Fig. 6. Pull-out load dependence on orientation angle to crack surface for straight fiber.

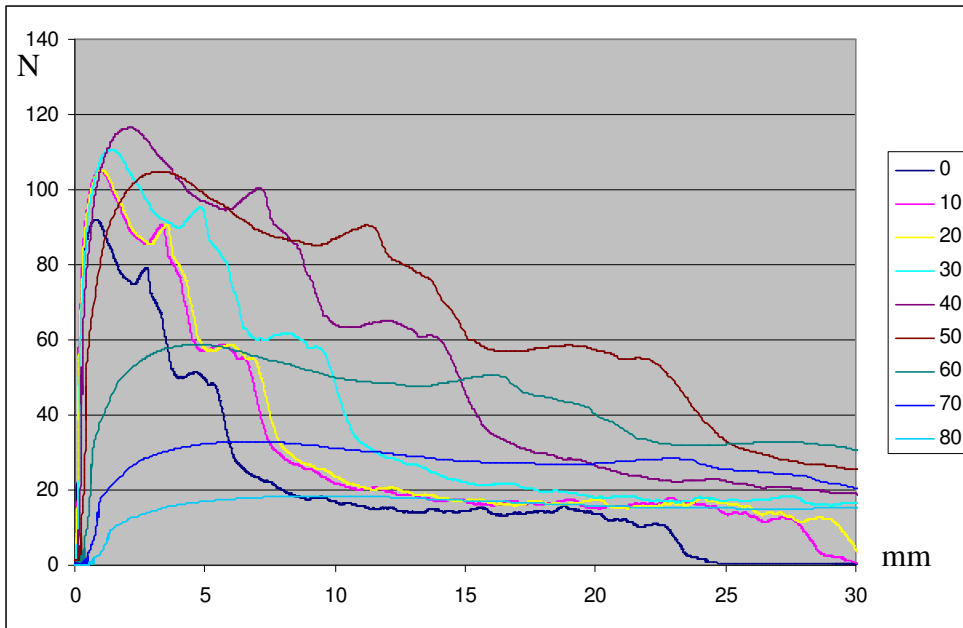


Fig. 7. Pull-out load dependence on orientation angle to crack surface for Dramix fiber.

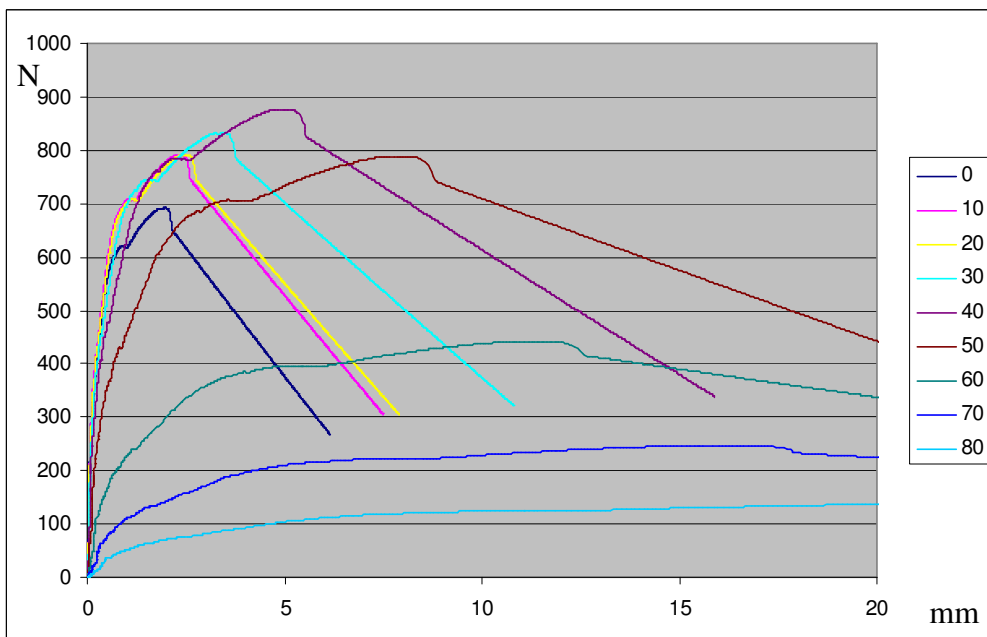


Fig.8. Pull-out load dependence on Tabix fiber orientation angle to crack surface.

### 3. Modeling results, comparison with experiments. Strength prediction

As it was described previously, the proposed model was applied for SFRC behavior prediction for materials with various fibre types and concentrations. In this case SFRC mixes with fibre concentration within the range from  $50 \text{ kg/m}^3$  to  $400 \text{ kg/m}^3$  were studied. Here is necessary to mention that mixes with fiber content more than  $100 \text{ kg/m}^3$  are technologically observed as SFRC with high fiber concentrations and traditionally have low workability. To evaluate the validity of the proposed model, parallel experimental tests were performed according to the same loading conditions. Fig. 9-12 represents some relevant modeling results also being compared with the experimental

data. Here the results for four different mixes have been presented.

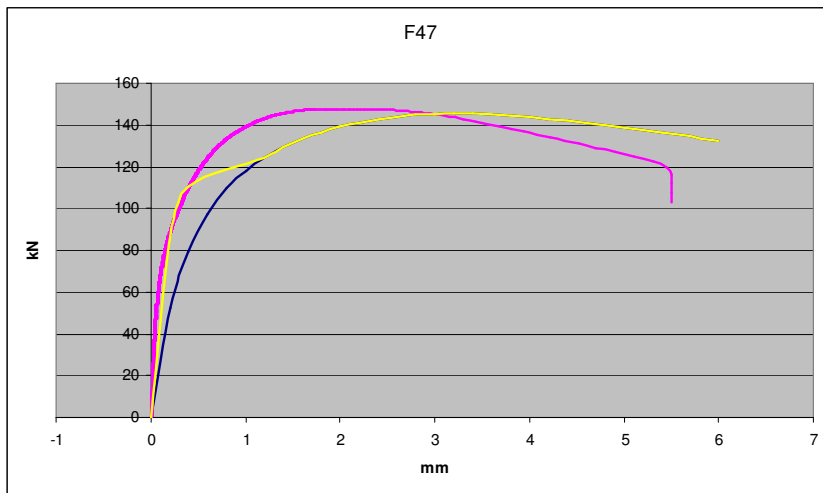


Fig. 9. — experimental curve, — theoretical curve, — smoothed theoretical curve. SFRC with “fibercocktail”, fibers: Tabix 50mm long,  $d=1\text{mm}$ : **179 kg/m<sup>3</sup>**, Dramix 30mm long,  $d=0,54\text{mm}$ : **90 kg/m<sup>3</sup>**, straight fibers 13mm long,  $d=0,16\text{mm}$ : **36 kg/m<sup>3</sup>**.

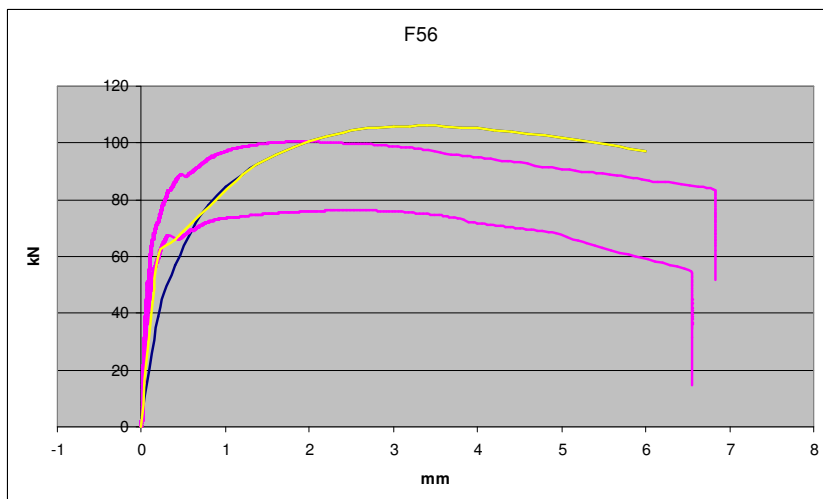


Fig. 10. — experimental curve, — theoretical curve, — smoothed theoretical curve. Fibers: Tabix 60mm long,  $d=1,0\text{mm}$ : **127 kg/m<sup>3</sup>**, Dramix 30mm long,  $d=0,54\text{mm}$ : **34 kg/m<sup>3</sup>**, Straight 13mm long,  $d=0,16\text{mm}$ : **24 kg/m<sup>3</sup>** Straight 6mm long,  $d=0,16\text{mm}$ : **10 kg/m<sup>3</sup>**.

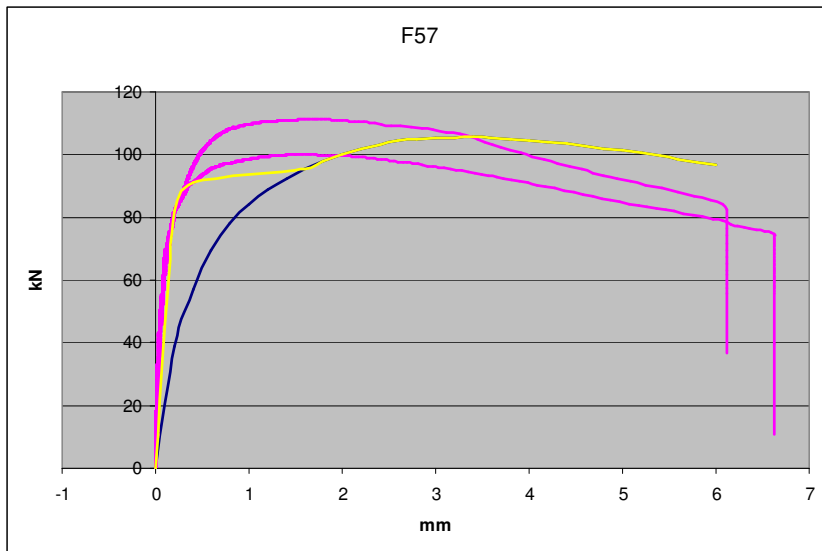


Fig. 11. — experimental curve, — theoretical curve, — smoothed theoretical curve. Fibers: Tabix 60mm long,  $d=1,0\text{mm}$ :  $127 \text{ kg/m}^3$ , Dramix 30mm long,  $d=0,54\text{mm}$ :  $34 \text{ kg/m}^3$ , Straight 13mm long,  $d=0,16\text{mm}$ :  $15 \text{ kg/m}^3$  Straight 6mm long,  $d=0,16\text{mm}$ :  $20 \text{ kg/m}^3$ .

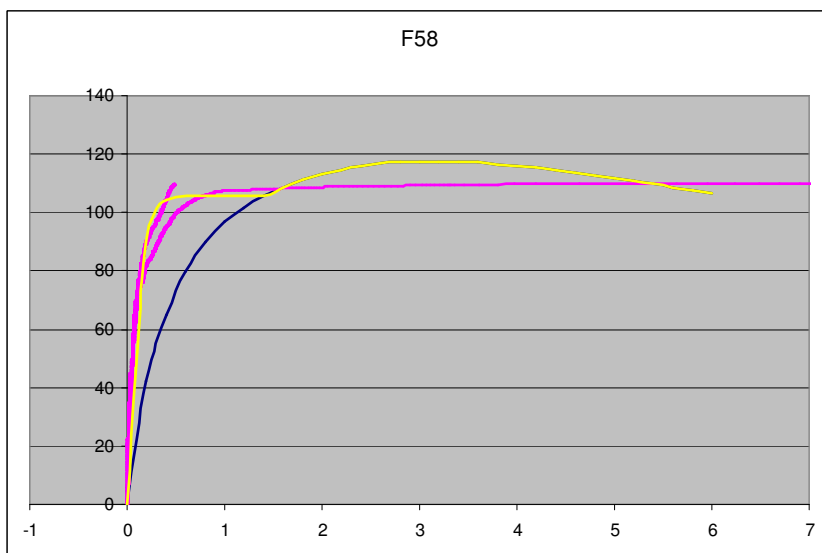


Fig. 12. — experimental curve, — theoretical curve, — smoothed theoretical curve. Fibres: Tabix 60mm long,  $d=1,0\text{mm}$ :  $115 \text{ kg/m}^3$ , Dramix 30mm long,  $d=0,54\text{mm}$ :  $86 \text{ kg/m}^3$ , Straight 6mm long,  $d=0,16\text{mm}$ :  $38 \text{ kg/m}^3$ .

As it is evident from all the plots the proposed model succeeded to agree with the experimental results regardless of the diversity of fiberconcretes were observed. Interpretation of this result can be the model basing on experimental detailed data for fiber pull-out, as the main micro-mechanical mechanism of non-linear SFRC post-cracking behavior. Very good modeling and experimental results agreement allow us to be certain predicting post cracking behavior of SFRC with different fiber content and type's combination. In Fig. 13 are shown the actual beam (crosssection size 15x15cm) fracture character with two different fiber combinations. Beams have ultimate strength 27,9MPa what is necessary to carry external bending moment 500kN\*m/m (with bulk safety factor 2.02 and size factor 0.6). Safety factor value was obtained experimentally.

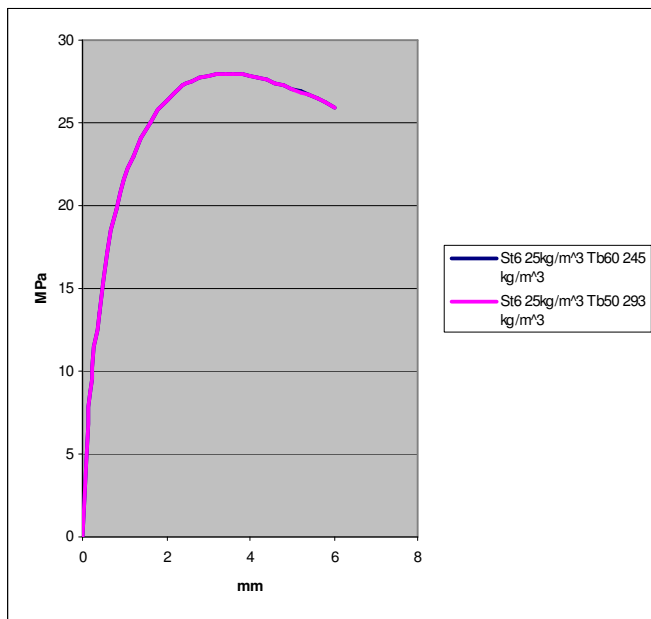


Fig. 13. . Predicted stress-deflection curves for two different SFRC with fibercocktails. Beam crosssection size 15x15cm; Strength  $[\sigma]=27,9\text{MPa}$ .

Figure 14 is showing stress –deflection curves for four different SFRC samples 15x15x60cm under 4 point bending. Each material needs to have bending strength 27.9MPa. Each material has only one type of steel fibers. Prediction is showing, its not possible to carry necessary load using fiberconcrete with 6mm long straight fibers (and concrete matrix with cube compressive strength in the range of 50-90MPa (concrete matrix was used in our experiments), because is necessary to add technologically not possible amount of fiber - not less then  $2671\text{kg/m}^3$  the same situation is with straight 13mm long fibers. At the same moment is possible to obtain necessary strength adding  $300\text{kg/m}^3$  Dramix 30mm long (with diameter 0.38mm) fibers or  $308\text{kg/m}^3$  Tabix 50mm long (with diameter 1mm) fibers. The same result may be obtained adding into concrete matrix fiber combinations:

- 1)  $173.4\text{kg/m}^3$  Tabix 60mm long (diameter 1mm),  
 $86.7\text{kg/m}^3$  Dramix 30mm (diameter 0.38mm),  
 $28.9\text{kg/m}^3$  straight 6mm (diameter 0.16mm).  
 Totally fibers:  $289\text{kg/m}^3$ ,  $V_f=3.7\%$ .
- 2)  $196.2\text{kg/m}^3$  Tabix 60mm long (diameter 1mm),  
 $98.1\text{kg/m}^3$  Dramix 30mm (diameter 0.38mm),  
 $32.7\text{kg/m}^3$  straight 6mm (diameter 0.16mm).  
 Totally fibers:  $327\text{kg/m}^3$ ,  $V_f=4.2\%$ .
- 3)  $198.1\text{kg/m}^3$  Tabix 60mm long (diameter 1mm),  
 $56.6\text{kg/m}^3$  Dramix 30mm (diameter 0.38mm),  
 $28.3\text{kg/m}^3$  straight 6mm (diameter 0.16mm).  
 Totally fibers:  $283\text{kg/m}^3$ ,  $V_f=3.6\%$ .



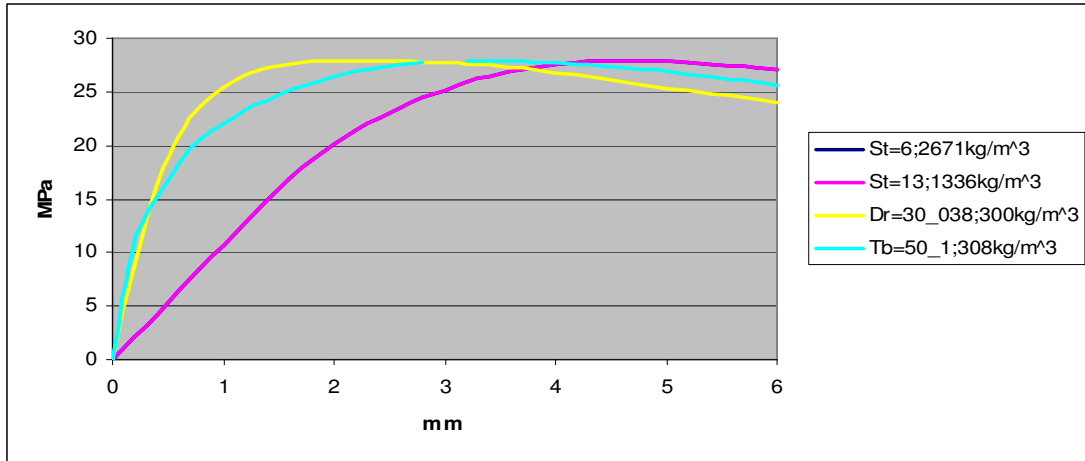


Fig. 14. Predicted stress-deflection curves for different SFRC containing one type of steel fibers and having strength  $[\sigma]=27,9\text{MPa}$  ( Beam crossection size  $15\times 15\text{cm}$ ).

At Fig. 15. are shown stress-deflection curves for SFRC having different concentrations of Tabix 50mm long ( $d=1\text{mm}$ ) fibers.

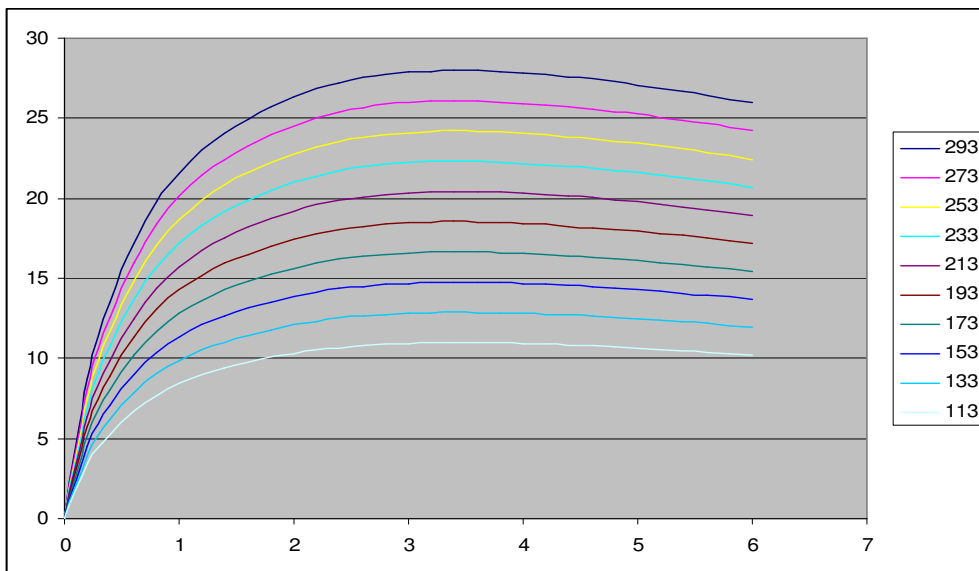


Fig. 15. Predicted stress-deflection curves for SFRC containing one type of steel fibers (Tabix  $l=50\text{mm}$ ,  $d=1\text{mm}$ ) and having strength  $[\sigma]=27,9\text{MPa}$  ( Beam crossection size is  $15\times 15\text{cm}$ ).

#### 4. Conclusions

Modeling results for the proposed SFRC (with fiber cocktails) beam mechanical behavior prediction model proved to be in a good agreement with experimentally obtained. Good agreement with the numerous experimental results confirms that the main non-linear

micro-mechanisms have been successfully recognized and applied in the proposed model. The validity of the proposed model has been experimentally proved for SFRC beams with fibre concentrations up to 400 kg/m<sup>3</sup>.

## **5. Acknowledgements**

The work presented in this paper has been done in the framework of FP6 STREP project SCOUT (project no. 516290).